Supplementary Information for:

Multiple States of Nitrile Hydratase from *Rhodococcus equi* TG328-2: Structural and Mechanistic Insights from EPR and DFT Studies†

Natalia Stein, Natalie Gumataotao, Natalia Hajnas, Rui Wu, K. P. Wasantha Lankathilaka, Uwe T. Bornscheuer, Dali Liu, Adam T. Fiedler, Richard C. Holz, and Brian Bennett

T1. X-ray Crystallography.

*Re*NHase-TG328-2 was concentrated to 20 mg/mL and exchanged into 50 mM HEPES buffer, pH 7.0, by ultrafiltration (Amicon Ultracel-50). Sitting drop vapor diffusion crystal screens (Emerald Biosystems Wizard 1 and 2; Hampton Research Index Screen 1 and 2, PEG/Ion 1 and 2, and Crystal Screen 1 and 2) with 10 mg mL^{-1} and 20 mg mL^{-1} *Re*NHase-TG328-2, were prepared (Art Robbins Crystal Gryphon robot) and incubated at 20 ˚C. A single cube-shaped crystal was obtained in 0.1 M bis(2-hydroxyethyl)amino-tris(hydroxymethyl)methane buffer, pH 5.5, with 2.0 M ammonium sulfate. The crystal was flash frozen with liquid nitrogen in a cryoprotectant solution containing the crystallization buffer and 40% glycerol. Crystallographic data were collected at the SBC beamline 19-ID at the Advanced Photon Source at Argonne National Laboratory. Alignment of the *Re*NHase TG328-2 sequence with that of the NHase from *Comamonas testosteroni* (*Ct*NHase) revealed that it is of similar length, shares broad sequence similarity (46% sequence identity and 60% similarity), and exhibits no sequence gaps. The structure was therefore determined by molecular replacement of the template structure from *Ct*NHase (PDB: 4FM4). The crystallographic, diffraction, and refinement parameters for *Re*NHase-TG328-2 are summarized in Table S1. The architecture of *Re*NHase-TG328-2 conforms to that of other Fe-type NHases, and the active site is buried at the interface of the α- and β-subunits. The active site Fe(III) ion in *Re*NHase-TG328-2 is identical to that in other Fe-type NHases in that it is six-coordinate and bound by two backbone amide nitrogen atoms, from αSer117 and αC118; three sulfur atoms, from αC113, αC116, and αC118; and a water/hydroxyl moiety (Figure 1A). Both αC116 and αC118 were clearly oxidized to cysteine sulfinic acids (Figure 1B).

Table S1. Data collection and refinement statistics of *Re*NHase.

Data Processing	
Space group	I23
Cell dimensions	
α, β, γ (°)	90.0; 90.0; 90.0
a, b, c (Å)	184.9; 184.9; 184.9
Resolution (Å)	41.4 - 2.57
[a]R_{merge} (%)	0.149 (0.485)[b]
I/σ (I)	11.5 (3.0)
Completeness (%)	99.8(99.0)
Multiplicity	6.2 (4.4)
No. Reflections	210086
No. Unique Reflections	33630
Refinement	
Average B factor (Å^2)	38.21
[c]R_{work}/[d]R_{free} (%)	17.24/22.08
No. of Atoms	
Non-solvent	6591
Water	236
[e]RMSD	
Bond length (Å)	0.003
Bond angle (°)	0.662
Ramachandran plot	
Most Favored (%)	96.98
Allowed (%)	2.39
Outliers (%)	0.63

[a] $R_{merge} = \Sigma|I_{obs}-I_{avg}|/\Sigma I_{avg}$

[b] The values for the highest resolution bind are in parentheses.

[c] $R_{work} = \Sigma|F_{obs}-F_{calc}|/\Sigma F_{obs}$.

[d] Five percent of the reflection data were selected at random as a test set and only these data were used to calculate R_{free}.

[e] RMSD, root mean square deviation

Table S2. Crystallographic bond distances at the active site of *Re*NHase-TG328-2.

Bonded Atoms	**Bond Distance (Å)**[a]
Fe-αCys116	2.10
Fe-O (H_2O or OH^-)	1.90
Fe-α(S)Cys113	2.19
Fe-α(N)Ser117	2.13
Fe-α(S)Cys118	2.31
Fe-α(N)Cys118	2.04

[a]Bond distances for the modeled active site are given to two decimal places; however, the diffraction resolution defines any given distance to a precision of only one decimal place.

Table S3. Metric parameters for geometry-optimized models of the FeNHase active site.

	$NHase^{Aq}$	$NHase^{BA}$	$NHaseOx^{Aq}$	$NHaseOx^{BA}$
Bond distances (Å)				
Fe1–S1	2.257	2.257	2.227	2.215
Fe1–S2	2.363	2.363	2.351	2.357
Fe1–S3	2.263	2.311	2.267	2.319
Fe1–N1	1.906	1.944	1.900	1.940
Fe1–N2	1.913	1.909	1.920	1.909
Fe–X	2.088	2.086	2.152	2.209
Bond angles (deg)				
S1-Fe-S2	85.0	79.5	89.6	86.9
S1-Fe-S3	89.1	88.6	90.1	89.8
S1-Fe-N1	101.7	96.8	100.4	95.5
S1-Fe-N2	97.4	96.6	97.4	96.7
S2-Fe-S3	95.4	98.2	98.0	100.1
S2-Fe-N1	167.8	167.7	163.7	165.4
S2-Fe-N2	84.9	84.6	81.4	81.0
S3-Fe-N1	94.8	93.5	94.9	94.3
S3-Fe-N2	173.5	174.5	172.4	173.5
N1-Fe-N2	84.2	84.1	84.5	84.5

Table S4. Optimized coordinates for $NHase^{Aq}$

N	1.097222	-1.122338	-1.134390
C	1.729908	-2.208652	-0.384967
C	1.136088	-2.303030	1.013848
O	1.553655	-3.119162	1.835734
C	3.257291	-2.118294	-0.342602
O	3.762263	-0.845195	0.006241
H	-1.054162	7.167252	0.003988
C	-1.337167	6.210763	-0.445743
N	-0.473041	5.155813	0.013527
C	-0.250233	4.852707	1.290743
N	-0.943434	5.474943	2.259860
N	0.706224	4.003694	1.625613
H	-6.166080	6.462912	-1.756467
C	-5.375461	5.874766	-2.217470
N	-4.885178	4.920664	-1.240571
C	-3.774964	4.176358	-1.400791
C	-1.804900	-3.256000	-1.305900
N	-2.991943	4.346652	-2.461065
N	-3.425547	3.272416	-0.502649
H	-2.172246	-4.253431	-1.043269
C	-2.479877	-2.216618	-0.433742
S	-2.054956	-0.472844	-0.809046
C	0.484869	-0.185370	-3.337304
C	0.844008	1.248688	-3.006914
S	0.093252	1.771847	-1.445925
C	1.155630	-1.251651	-2.478075
O	1.700827	-2.192829	-3.052181
O	1.034522	2.894479	-0.960485
O	-1.255892	2.415300	-1.829265
N	0.141195	-1.434351	1.219586
C	-0.389498	-1.348066	2.560352
C	-1.558352	-0.392715	2.579383
S	-1.115503	1.140356	1.693673
O	0.073689	1.718123	2.639068
H	-1.854265	-0.107211	3.590617
H	0.378381	-1.006007	3.266044

Fe	0.013853	0.000143	-0.040085
O	1.698124	0.790884	0.907653
H	-0.599699	-0.325407	-3.282683
H	0.492763	1.960533	-3.757926
H	1.520053	-3.166256	-0.878146
H	3.651784	-2.355524	-1.330355
H	3.594648	-2.887365	0.363438
H	-1.225763	6.299267	-1.522739
H	-2.392290	6.021192	-0.225489
H	-0.029738	4.520943	-0.654837
H	-1.836048	5.894691	2.071698
H	-0.735403	5.229751	3.213518
H	2.024493	1.529662	0.373328
H	0.444788	3.202771	2.281102
H	-4.583351	6.565895	-2.510800
H	-5.780768	5.388366	-3.110338
H	-5.538941	4.604354	-0.543477
H	-3.337537	4.814134	-3.280172
H	-2.190068	3.700834	-2.545567
H	-3.978700	3.065454	0.311028
H	-2.624318	2.657133	-0.730853
H	-3.565510	-2.263046	-0.568882
H	-2.262603	-2.420500	0.615611
H	-0.711461	-2.333381	2.920376
H	-2.423585	-0.784520	2.044128
H	1.918002	1.378558	-2.862805
H	0.798991	-0.395313	-4.360633
H	1.171184	3.616737	0.804334
H	3.173977	-0.456985	0.667964
H	1.292007	1.163730	1.755531
H	-0.725794	-3.243349	-1.162191
H	-2.007772	-3.081336	-2.364824

Table S5. Optimized coordinates for $NHase^{BA}$

N	1.157323	-1.051372	-1.079556
C	1.729908	-2.208652	-0.384967
C	1.281826	-2.254815	1.067443
O	1.688977	-3.131449	1.828909
C	3.247527	-2.262301	-0.544015
O	3.857615	-1.007524	-0.304011
H	-1.053367	7.185442	-0.035285
C	-1.337167	6.210763	-0.445743
N	-0.457160	5.175603	0.018420
C	-0.250233	4.852707	1.290743
N	-0.899842	5.506065	2.271036
N	0.641909	3.928526	1.608648
H	-6.150716	6.481344	-1.754279
C	-5.375461	5.874766	-2.217470
N	-4.859547	4.954350	-1.222879
C	-3.774964	4.176358	-1.400791
C	-1.804900	-3.256000	-1.305900
N	-3.012544	4.302704	-2.481062
N	-3.428051	3.274860	-0.498759
H	-2.029656	-4.283457	-0.999202
C	-2.156485	-2.304717	-0.181893
S	-1.911579	-0.535692	-0.600677
C	0.398643	-0.156761	-3.267094
C	0.833150	1.248458	-2.927857
S	0.058967	1.838464	-1.410988
C	0.979449	-1.268682	-2.410556
O	1.257472	-2.324223	-2.974838
O	0.869646	3.100000	-1.092894
O	-1.359350	2.272165	-1.849009
N	0.379726	-1.315064	1.367682
C	-0.185729	-1.303395	2.696751
C	-1.475042	-0.512880	2.685829
S	-1.219788	1.060219	1.788991
O	-0.321754	1.840021	2.911763
H	-1.807874	-0.234832	3.687129
H	0.511705	-0.871215	3.425054
Fe	0.134872	0.098141	0.108276
O	1.857630	1.011438	0.849337
H	-0.692798	-0.237298	-3.227157
H	0.548593	1.977693	-3.690529
H	1.358003	-3.134488	-0.836695

H	3.483683	-2.613581	-1.554465
H	3.646295	-2.975922	0.179059
H	-1.252212	6.267480	-1.527511
H	-2.385752	6.020082	-0.193080
H	-0.023297	4.519696	-0.650720
H	-1.748591	6.007124	2.078792
H	-0.747740	5.199699	3.217945
C	2.538352	1.172333	1.875442
H	0.325336	3.213913	2.310130
H	-4.591532	6.554012	-2.557734
H	-5.806842	5.358592	-3.080960
H	-5.496215	4.666702	-0.498051
H	-3.343478	4.792616	-3.292649
H	-2.230893	3.630673	-2.567179
H	-3.964165	3.095830	0.332806
H	-2.646286	2.636005	-0.744354
H	-3.213802	-2.403307	0.084278
H	-1.565453	-2.537106	0.701140
H	-0.374468	-2.328368	3.039086
H	-2.277185	-1.033874	2.167411
H	1.906831	1.321690	-2.746318
H	0.704381	-0.387506	-4.288849
H	1.075326	3.486624	0.794743
H	3.215041	-0.344800	-0.597471
C	4.020380	1.296966	1.774520
H	-0.751476	-3.202888	-1.575218
H	-2.385488	-3.036620	-2.204979
O	2.047347	1.273532	3.061218
H	0.976487	1.385780	3.034444
H	4.453371	1.633459	2.713495
H	4.265607	1.994699	0.972829
H	4.426885	0.326478	1.479691

Table S6. Optimized coordinates for $NHaseOx^{Aq}$

N	1.142676	-1.091688	-1.125564
C	1.729908	-2.208652	-0.384967
C	1.125014	-2.296759	1.010710
O	1.502245	-3.140992	1.821373
C	3.261395	-2.208026	-0.347583
O	3.850709	-0.965305	-0.028796
H	-1.072320	7.179561	-0.012961
C	-1.337167	6.210763	-0.445743
N	-0.441361	5.181708	0.017350
C	-0.250233	4.852707	1.290743
N	-0.981031	5.435014	2.255906
N	0.738504	4.032061	1.614993
H	-6.139762	6.491125	-1.748804
C	-5.375461	5.874766	-2.217470
N	-4.879262	4.929972	-1.229811
C	-3.774964	4.176358	-1.400791
C	-1.804900	-3.256000	-1.305900
N	-3.040514	4.321765	-2.507931
N	-3.382032	3.301194	-0.503240
H	-2.221346	-4.227218	-1.020329
C	-2.445224	-2.162426	-0.475332
S	-1.956662	-0.438738	-0.868879
C	0.576855	-0.126768	-3.334203
C	0.955758	1.297885	-2.987890
S	0.205294	1.826892	-1.426726
C	1.206976	-1.214361	-2.472020
O	1.731061	-2.168705	-3.041832
O	1.201455	2.890846	-0.911488
O	-1.107010	2.531325	-1.804872
N	0.151353	-1.400887	1.224670
C	-0.457001	-1.401431	2.542019
C	-1.571675	-0.375560	2.602641
S	-0.958041	1.113762	1.779621
O	0.161161	1.609966	2.732599
H	-1.855137	-0.094431	3.618331
H	0.290073	-1.180281	3.313776
Fe	0.057850	0.034976	-0.045987
O	1.853491	0.781275	0.876853
H	-0.510812	-0.247366	-3.304845
H	0.616696	2.020476	-3.734098
H	1.470321	-3.152151	-0.882435

H	3.636173	-2.493960	-1.329950
H	3.550089	-2.981531	0.375216
H	-1.242350	6.279470	-1.525720
H	-2.383212	5.995069	-0.210157
H	0.026232	4.577818	-0.657686
H	-1.908240	5.755586	2.033918
H	-0.863016	5.074149	3.189358
H	2.128748	1.552456	0.355298
H	0.555299	3.322395	2.340513
H	-4.573244	6.535980	-2.547850
H	-5.817209	5.378259	-3.087595
H	-5.530778	4.609147	-0.532008
H	-3.469184	4.659617	-3.351932
H	-2.218950	3.711609	-2.591561
H	-3.747977	3.209999	0.431226
H	-2.549650	2.730742	-0.706199
H	-3.529236	-2.163745	-0.630882
H	-2.262039	-2.346826	0.583937
H	-0.858039	-2.393196	2.783895
H	-2.452469	-0.672565	2.033506
H	2.030985	1.411382	-2.840794
H	0.908368	-0.335298	-4.352397
H	1.195577	3.618828	0.798680
H	3.274664	-0.505404	0.596663
H	1.519010	1.100382	1.749844
H	-0.728299	-3.289022	-1.146469
H	-1.984518	-3.104942	-2.372633
O	-2.085333	2.122377	1.705852

Table S7. Optimized coordinates for $NHaseOx^{BA}$

N	1.195861	-1.033589	-1.076147
C	1.729908	-2.208652	-0.384967
C	1.329140	-2.211452	1.079220
O	1.713801	-3.094318	1.841307
C	3.245652	-2.318098	-0.577683
O	3.889151	-1.067450	-0.417080
H	-1.030888	7.177083	-0.032763
C	-1.337167	6.210763	-0.445743
N	-0.487669	5.153939	0.022442
C	-0.250233	4.852707	1.290743
N	-0.911926	5.480694	2.280685
N	0.725489	4.002604	1.585858
H	-6.128272	6.506705	-1.750979
C	-5.375461	5.874766	-2.217470
N	-4.848358	4.970714	-1.209356
C	-3.774964	4.176358	-1.400791
C	-1.804900	-3.256000	-1.305900
N	-3.064656	4.269730	-2.526139
N	-3.390772	3.301076	-0.497192
H	-2.025351	-4.279362	-0.982585
C	-2.015395	-2.305132	-0.148492
S	-1.801074	-0.532090	-0.567354
C	0.463048	-0.123923	-3.269330
C	0.910870	1.276574	-2.925666
S	0.113078	1.885567	-1.427422
C	1.015997	-1.246011	-2.408230
O	1.277287	-2.308356	-2.967562
O	0.915933	3.153860	-1.115734
O	-1.300457	2.290416	-1.878671
N	0.474404	-1.227159	1.401309
C	-0.104124	-1.260959	2.731767
C	-1.347979	-0.393274	2.772667
S	-0.891865	1.147814	1.932669
O	0.082875	1.749558	2.989065
H	-1.658052	-0.122382	3.783032
H	0.613249	-0.916172	3.486383
Fe	0.199277	0.143448	0.100921
O	2.083090	1.113265	0.725153
H	-0.629849	-0.189372	-3.245351
H	0.647192	2.005551	-3.696008
H	1.305914	-3.123976	-0.810666

H	3.447944	-2.724332	-1.573951
H	3.644243	-3.003309	0.171952
H	-1.247765	6.260593	-1.527856
H	-2.391995	6.049585	-0.199508
H	-0.022067	4.524935	-0.650899
H	-1.835434	5.833152	2.094718
H	-0.763848	5.131819	3.214482
C	2.904461	1.252027	1.631898
H	0.567256	3.332694	2.353410
H	-4.586392	6.526771	-2.595437
H	-5.839437	5.344179	-3.055469
H	-5.484325	4.676699	-0.485812
H	-3.482995	4.640675	-3.360980
H	-2.274440	3.615246	-2.615371
H	-3.734472	3.246642	0.448322
H	-2.593208	2.686317	-0.725165
H	-3.039175	-2.392380	0.229424
H	-1.340832	-2.546855	0.669606
H	-0.354514	-2.291715	3.006890
H	-2.179193	-0.820880	2.215693
H	1.982274	1.338237	-2.727349
H	0.777908	-0.358756	-4.287431
H	1.158121	3.565786	0.769201
H	3.256793	-0.412117	-0.748831
C	4.353300	1.459831	1.348961
H	-0.784411	-3.227935	-1.686017
H	-2.471664	-3.016849	-2.138027
O	2.588149	1.253585	2.897246
H	1.581337	1.271172	2.995159
H	4.887115	1.800694	2.233024
H	4.460472	2.180586	0.538038
H	4.764233	0.510630	0.995062
O	-2.093612	2.047548	1.783488

Table S8. Optimized coordinates for NHase^{BuBA}

N	1.054750	-1.121363	-1.087799
C	1.729908	-2.208652	-0.384967
C	1.072522	-2.447546	0.967974
O	1.471170	-3.302584	1.751948
C	3.238982	-2.001678	-0.274942
O	3.629611	-0.772175	0.276328
H	-0.975708	7.224004	-0.181255
C	-1.337167	6.210763	-0.445743
N	-0.435136	5.183617	0.013180
C	-0.250233	4.852707	1.290743
N	-0.942193	5.492906	2.261649
N	0.590028	3.876244	1.602878
H	-6.095360	6.552678	-1.735984
C	-5.375461	5.874766	-2.217470
N	-4.838165	4.984560	-1.213325
C	-3.774964	4.176358	-1.400791
C	-1.804900	-3.256000	-1.305900
N	-3.067960	4.205668	-2.534020
N	-3.367080	3.338715	-0.456213
H	-2.178771	-4.274924	-1.091978
C	-2.559701	-2.240160	-0.464012
S	-2.132725	-0.485658	-0.759695
C	0.415879	-0.112398	-3.251729
C	0.824584	1.291114	-2.844223
S	0.031348	1.783055	-1.312131
C	1.082963	-1.219561	-2.440627
O	1.611971	-2.143185	-3.050157
O	0.850331	3.009156	-0.888900
O	-1.352000	2.292226	-1.763056
N	0.018488	-1.638333	1.179966
C	-0.565132	-1.691397	2.494575
C	-1.710009	-0.703304	2.594404
S	-1.251435	0.862889	1.800837
O	-0.024023	1.311179	2.876539
H	-2.002147	-0.475366	3.632651
H	0.190471	-1.476826	3.278507
Fe	-0.034062	-0.077688	0.070066
O	1.438739	0.651949	1.122462
H	-0.683282	-0.220778	-3.185571
H	0.526222	2.068980	-3.568639
H	1.605137	-3.141800	-0.965822

H	3.664821	-2.102995	-1.290721
H	3.627297	-2.835694	0.340253
H	-1.391279	6.148439	-1.540861
H	-2.359040	6.075578	-0.044997
H	0.000035	4.498724	-0.647034
H	-1.417788	6.360734	2.050429
H	-0.644601	5.368313	3.222720
H	0.470659	3.365163	2.479131
H	-4.573634	6.497116	-2.650333
H	-5.895677	5.334960	-3.031568
H	-5.426212	4.771341	-0.416824
H	-3.450569	4.613156	-3.376964
H	-2.277042	3.519462	-2.582150
H	-3.845552	3.240881	0.429787
H	-2.574535	2.684955	-0.725974
H	-3.642148	-2.293317	-0.687106
H	-2.433745	-2.481594	0.604487
H	-0.939789	-2.707856	2.729675
H	-2.600491	-1.022292	2.030382
H	1.906040	1.372313	-2.645601
H	0.717071	-0.288036	-4.296231
H	0.939828	3.319380	0.784690
H	2.843388	-0.230736	0.507114
H	-0.728304	-3.227594	-1.079866
H	-1.934290	-3.057338	-2.384259
B	1.292572	0.991150	2.387385
C	2.467705	1.163088	3.440912
C	3.181744	-0.169452	3.714955
H	4.034243	-0.037729	4.405223
H	3.562358	-0.602426	2.774227
H	2.500627	-0.912084	4.166310
H	2.095376	1.608216	4.383015
H	3.201958	1.875479	3.017572

Table S9. Comparison of experimental and computed g-values for $[Fe^{3+}(ADIT)(ADIT\text{-}X)]^{+/2+}$ complexes.[a]

complex	method [b]	g_1	g_2	g_3	g_1-g_3	rms deviation [c]
$[Fe^{3+}(ADIT)(ADIT)]^{+}$	exper	2.17	2.11	1.99	0.180	
	CP-SCF	2.139	2.095	2.042	0.097	0.036
	Taylor/DFT	2.156	2.125	1.987	0.169	0.012
$[Fe^{3+}(ADIT)(ADIT\text{-}H)]^{2+}$	exper	2.22	2.15	1.97	0.250	
	CP-SCF	2.160	2.121	2.041	0.118	0.056
	Taylor/DFT	2.201	2.162	1.979	0.222	0.014
$[Fe^{3+}(ADIT)(ADIT\text{-}O)]^{2+}$	exper	2.20	2.16	1.98	0.220	
	CP-SCF	2.147	2.122	2.037	0.110	0.050
	Taylor/DFT	2.172	2.160	1.980	0.192	0.016
$[Fe^{3+}(ADIT)(ADIT\text{-}OH)]^{2+}$	exper	2.24	2.15	1.97	0.270	
	CP-SCF	2.164	2.118	2.036	0.127	0.061
	Taylor/DFT	2.202	2.159	1.970	0.232	0.023

[a] The complexes and experimental g-values were originally reported in Lugo-Mas *et al*., *J. Am. Chem. Soc*. **2006**, *128*, 11211-11221. See Scheme S1 for structures of the complexes.

[b] exp = experimental; see main text for details regarding the CP-SCF and Taylor/DFT methods.

[c] Root-mean-square deviation between computed and experimental g-values.

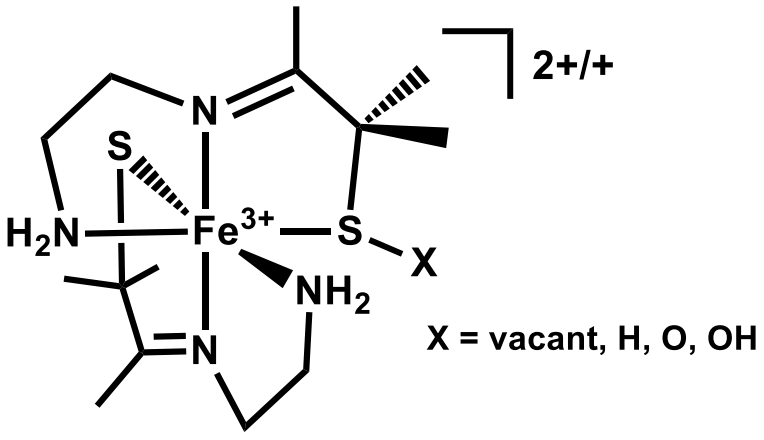

Scheme S1. Structure of the $[Fe^{3+}(ADIT)(ADIT\text{-}X)]^{+/2+}$ complexes.

T2. pH-Dependence of NHase. A sample, from which the butyric acid N*a* signal had been extinguished by turning over the enzyme with methacrylonitrile followed by buffer exchange, was found to substantially exhibit the active-resting N*b* signal at pH 7.6 (50 mM HEPES) (**Figure S1**, Trace C). Aliquots of the sample were buffer-exchanged into 50 mM MES, pH 6.3 (S1 A); 50 mM MOPS, pH 7.0 (S1 B); and Tricine, pH 8.0 (S1 D); respectively. The pH-dependence of the EPR signals of *Re*NHase-TG328-2 differed from that reported for *Re*NHase-N771[13] under their respective conditions. First, the pH-dependence of the resonant field for the dominant g_1 turning point was much smaller for *Re*NHase-TG328-2, increasing by only about 0.002 between pH 6.3 and pH 8.0, than for *Re*NHase-N771 where shifts of 0.02 were observed. Second, a signal that exhibited its largest observed intensity at pH 6.3 was observed, with a g_1 value (2.181) almost indistinguishable from that for the oxidized N*c* species. However, a difference spectrum (Figure S1 F) indicated a g_2 for this species of 2.125 at pH 7.0, compared to 2.114 for the N*c* species at pH 7.5. It is unclear whether the low-pH species is indeed an oxidized species (i.e. with two cysteine-sulfinate moieties), and thus whether low pH promotes oxidation, or whether this represents a new species that differs due to protonation of an active site moiety. Also of interest is the observation that in the relatively very 'clean' (i.e. uncontaminated with other signals) N*b* signal obtained by difference in Figure S1 E, there is a barely resolved symmetric splitting of the g_3 feature of about 8 G. This feature was also observed in some samples prepared in ^2H_2O, suggesting the presence of a non-exchangeable proton superhyperfine coupling.

Figure S1 (next page). (A-D) EPR spectra from NHase at pH 6.3 (A); pH 7.0 (B); ph 7.6 (C); and pH 8.0 (D). To generate Trace E, varying proportions of Trace B were subtracted from Trace C until the spectrum most closely approached a single species; the resultant is shown amplified by a factor of 2.7. To generate Trace F, varying proportions of Trace C were subtracted from Trace B until the spectrum most closely approached a single species; the resultant is shown amplified by a factor of 8.0. Spectra were recorded at 9.6 GHz, 30 K, 0.1 mW microwave power.

Figure S1.

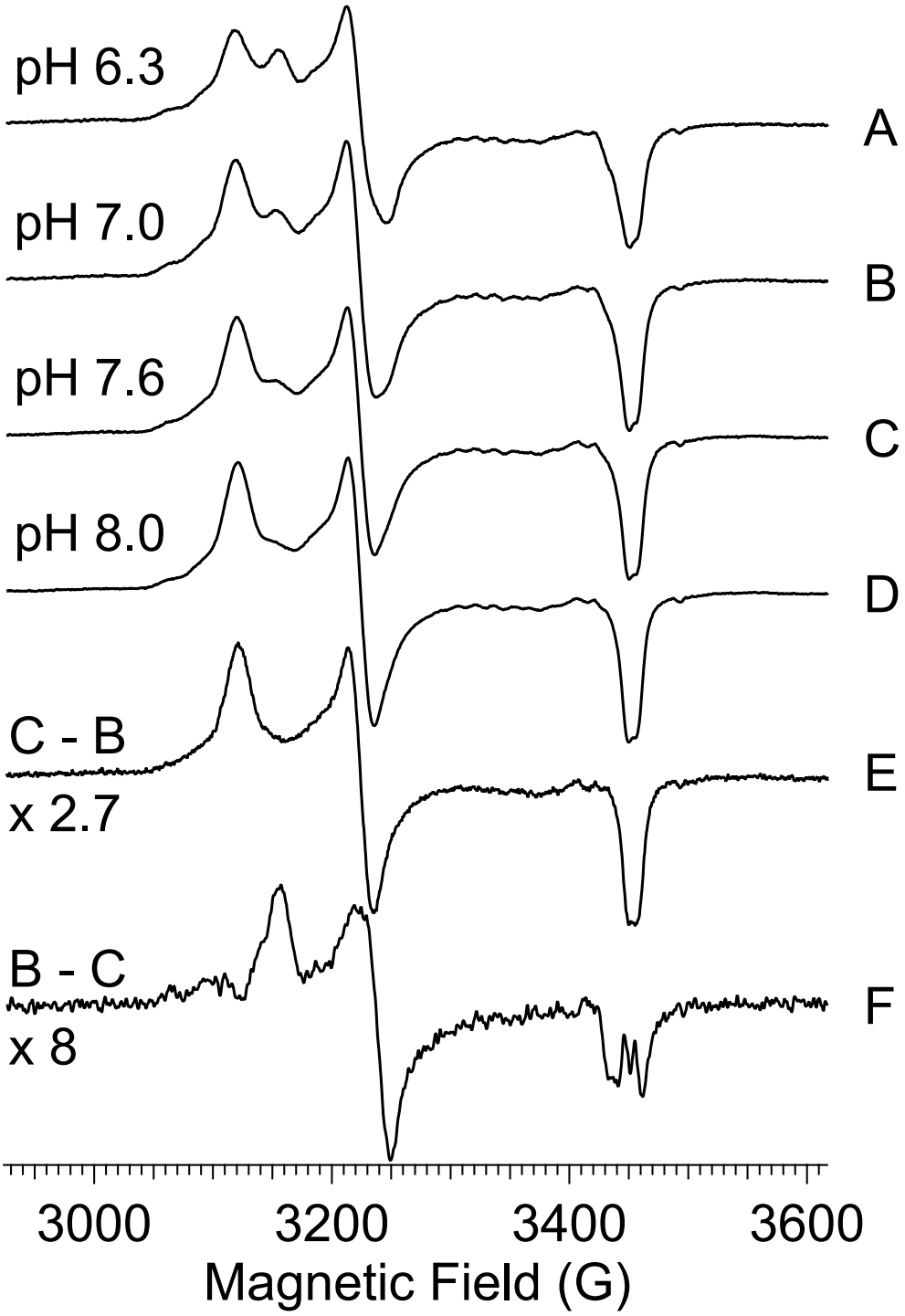
pH 6.3
A
pH 7.0
B
pH 7.6
C
pH 8.0
D
C - B
x 2.7
E
B - C
x 8
F
3000
3200
3400
3600
Magnetic Field (G)

Text T3. Consideration of the Assignments of N*a* and N*b* in the Light of ENDOR Data. (References below)

The assignment of N*a* to a carboxylic acid complex of NHase is supported by widespread EPR data including (i) its elucidation by addition of butyric acid, (ii) its elimination by displacement, and (iii) its diminution or non-appearance in preparations that either avoided or scrupulously removed butyric acid. That the butyric acid form has no catalytic activity has been demonstrated, and the contention that the butyric acid complex includes replacement of the apical water/hydroxyl, and monodentate binding to the metal ion, is supported by (i) X-ray crystallographic data, and (ii) the observation that the N*a* form can be converted to the active N*b* form by cryogenic photolysis and subsequently reformed by annealing. Circumstantial supporting evidence comes from DFT, particularly reproduction of the very high g_1 value.

Earlier studies have identified two exchangeable protons by ^{1}H- and ^{2}H-ENDOR at one single-crystal like orientation (g_1). Comparison of ^{1}H hyperfine couplings (6 and 4.5 MHz), ^{2}H quadrupolar coupling estimations (both at g_1) and ^{17}O-ENDOR parameters (at g_3), from Fe^{3+} in NHase were initially assigned to an Fe- bound water molecule. This assignment of Fe-OH_2 rather than Fe-OH was reversed when the implicit TRIPLE effect in Mims ENDOR indicated that the two proton hyperfine couplings were of opposite sign and that, therefore, the two observed reversible protons must be due to discrete moieties[5] By comparison to the $[4Fe4S]^{+}$ cluster in aconitase, which bears very little structural or, indeed, electronic relationship to the active site of NHase other than exhibiting an $S = {}^{1}/_{2}$ EPR signal, one of the protons was assigned to an Fe-bound hydroxyl and the other to some other nearby species (a Cys-S...H-N species was tentatively proposed).[5,48]

The apparent contradiction with our assignment of N*a* arises because it the reported ENDOR conditions appear to indicate that the ENDOR data collected at g_1 could only have arisen from the N*a* carboxylic acid EPR species. (Data collected at g_3 could have been due to any one of a number of species - the EPR spectrum itself was not reported in the communications of the ENDOR data, though earlier work on that system by coauthors indicated that the preparations were predominantly in the N*a* state. Nevertheless, any sample manipulation - buffer exchange, concentration by ultrafiltration, addition of

cryoprotectant, sustained exposure to oxygen - certainly has the potential to significantly change the complement of EPR species, as the present work has clearly shown). Given the overwhelming evidence from multiple sources that favors our assignment of N*a*, we must therefore question the earlier assignment of one of the two protons to an Fe-bound hydroxyl. Given that one of the protons (the assignment of one to the hydroxyl and the other to an ill-defined nearby species appears arbitrary) must be due to some non-Fe-bound species, and that the couplings suggest that they are, in fact, chemically very similar other than they must not be coupled to each other, it is not a stretch of the imagination to suggest that *both* protons are due to a species other than a direct iron ligand.

Our own ENDOR investigation was limited by resources and was therefore focused on ascertaining the origin of the EPR-observable hyperfine interaction. The non-exchangeable proton couplings that we observed, 24 MHz from an essentially isotropically-coupled ^{1}H and 10 MHz from a more anisotropically coupled one, are far larger than that assigned to the hydroxyl and are most likely due to cysteine β protons. We also saw a number of more weakly coupled protons with couplings in the range of those observed in the earlier work. Both our data, then, and the recognition in the earlier work that at least one of the observed protons in that study must come from the protein scaffold, indicate that there are likely a number of candidates for the previously-observed 5.5 and 6 MHz protons other than a bound hydroxyl in the N*a* species.

If, after further work, the assignments of the earlier study were to be confirmed and a hydroxyl ligand is indeed present in the N*a* species of NHase, then a number of interesting questions arise. That N*a* is a complex with carboxylic acid seems beyond question. However, the crystallographic evidence for the monodentate binding of carboxylate and replacement of water/hydroxyl was for the Co-type NHase. To date, the Fe- and Co-type enzymes have displayed a remarkable level of structural and functional identity, but it is perhaps possible that the carboxylate complexes of these two enzyme forms differ in terms of binding to Fe, i.e. that carboxylate does not bind directly to Fe but does bind to Co. Alternative explanations would then have to be found for (i) the similarity of the reversible inhibition of Co-NHase and Fe-NHase by butyric acid, (ii) the mechanisms of oxidation prevention in each by butyric acid, (iii)

the reversible cryo-photolysis conversion of N*a* into N*b* in Fe-NHase, and (iv) the Taylor-DFT calculations.

A final question is the origin of the ^{17}O-ENDOR resonances.[48] These data were collected at g_3 and our EPR data herein have shown that there is overlap of multiple EPR signals at the corresponding field value that will persist at the 35 GHz used for those earlier ENDOR studies. As noted above, while an earlier reported EPR spectrum of *Rh*NHase-R312 with butyric acid[13] appears to be largely due to a single species, no EPR data were presented in the communications of the ENDOR work, and the EPR spectrum is highly sensitive to sample manipulation. If the ^{17}O resonances are indeed due to the N*a* species, then possible sources can be considered. As with the proton data, a bound hydroxyl may be a possibility but throws up a number of contradictions that have no obvious avenue for reconciliation. In the crystallographically-characterized type I butyric acid conformation, one carboxylic oxygen is clearly bound to Co, while the other carboxylic oxygen atom is hydrogen bonded (2.9 Å) to the active site tyrosine (βTyr68 of 1UGP). The second carboxylic oxygen atom in the type II complex is only 1.4 Å from the sulfenic oxygen atom of αCys113 [of 1UGP; corresponding to αCys118 of *Re*NHase-TG328-2 (Scheme 3)]. Given the acknowledged uncertainty in the interpretation of the butyric acid density, and "blobs of electron density" that could not be interpreted in the active site of complexes with other inhibitors, one can perhaps not categorically rule out the presence of disordered water in the vicinity of the metal ion as the source of both the exchangeable ^{1}H- and ^{17}O-ENDOR resonances observed earlier.[5,48] An alternative explanation for the observation of solvent-derived ^{17}O coupled to the Fe^{3+} in the reversible complex of NHase with butyric acid is through exchange with either the sulfenic acid oxygen or with the a carboxylic acid oxygen. The oxygen transferred to substrate by nitrile hydratase is known to be protein-derived rather than directly donated by solvent.[49] Therefore, exchange of the sulfenic oxygen must take place, at least during reconstitution of the active site during catalysis. Oxygen exchange in other cysteine-sulfenic acid enzymes has been observed.[50] In catalytically inactive systems, nucleophile- and acid-catalyzed ^{18}O-exchange in sulfenic acids has been characterized,[51] and the observed binding of carboxylic

oxygen to the sulfenic oxygen in NHase[45] renders this an intriguing possible alternative mechanism of oxygen exchange in the enzyme. Finally, the direct exchange of oxygen in carboxylic acids has been characterized; the rate for naked butyric acid would be presumed to be slow based on these data, but unpredictable in the NHase active site environment.

References for T3.

5. Doan, P. E.; Nelson, M. J.; Jin, H.; Hoffman, B. M., *J. Am. Chem. Soc.* **1996,** *118* (29), 7014-7015.
45. Miyanaga, A., Fushinobu, S., Ito, K., Shoun, H., Wakagi, T. (2004) Mutational and Structural Analysis of Cobalt-Containing Nitrile Hydratase on Substrate and Metal Binding. *Eur. J. Biochem. 271*, 429-438.
48. Jin, H., Turner, I.M., Nelson, M.J., Gurbiel, R.J., Doan, P.E., Hoffman, B.M. (1993) Coordination Sphere of the Ferric Ion in Nitrile Hydratase. *J. Am. Chem. Soc. 115*, 5290-5291.
49. Nelp, M.T., Song, Y., Wysocki, V.H., Bandarian, V. (2016) A Protein-Derived Oxygen is the Source of the Amide Oxygen of Nitrile Hydratases. *J. Biol. Chem. 291*, 7822-7829.
50. Allison, W.S., Benitez, L.V. (1972) An Adenosine Triphosphate-Phosphate Exchange Catalyzed by a Soluble Enzyme Couple Inhibited by Uncouplers of Oxidative Phosphorylation. *Proc. Natl. Acad. Sci. USA 69*, 3004-3008.
51. Kice, J.L., Cleveland, J.P. (1972) Nucleophilic Substitution Reactions Involving Sulfenic Acids and Sulfenyl Derivatives. the Nucleophile- and Acid-Catalyzed Oxygen-18 Exchange of Phenyl Benzenethiosulfinate. *J. Am. Chem. Soc. 95*, 104-109.